# Morphologies of Bottle-Brush Block Copolymers

**ARTICLE** *in* ACS MACRO LETTERS · OCTOBER 2014

Impact Factor: 5.76 · DOI: 10.1021/mz500580f



**2 AUTHORS:**

Alexandros Chremos
National Institute of Standards and Technol…
**30** PUBLICATIONS **269** CITATIONS

SEE PROFILE

Panagiotis Theodorakis
Imperial College London
**40** PUBLICATIONS **279** CITATIONS

SEE PROFILE

ACS Macro Letters

Letter

pubs.acs.org/macroletters

# Morphologies of Bottle-Brush Block Copolymers

Alexandros Chremos* and Panagiotis E. Theodorakis

Department of Chemical Engineering, Imperial College London, South Kensington Campus, SW7 2AZ London, United Kingdom

Supporting Information

**ABSTRACT:** We investigate the self-assembly of bottle-brush block copolymers into well-defined periodic morphologies by using molecular dynamics simulations of a bead-spring model. The microphase separation is driven by the chemical incompatibility between the different blocks of side chains leading to the formation of two- and three-domain lamellae and hexagonally packed cylinders. The molecular asymmetry required for the formation of cylindrical domains is not introduced by the difference in volume fractions, but by the asymmetry of the side chain lengths. Such behavior deviates significantly from what is typically known for linear block copolymers. The obtained morphology maps provide a genuine way of understanding the role of molecular architecture in achieving experimentally desired structures for nanoporous and photonic materials based on the self-assembly of bottle-brush block copolymers.

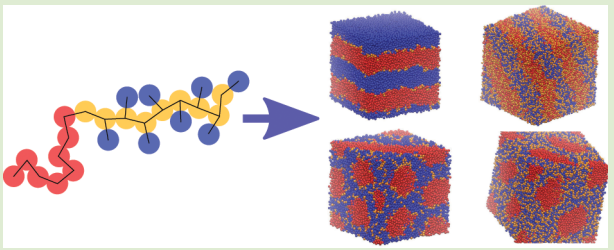

Materials with well-defined periodic morphologies are used in a diverse and expanding range of practical applications such as drug delivery,[1] microelectronics,[2] and other advanced materials.[3] A cost-effective, robust, and scalable way of generating complex multidomain morphologies is through the self-assembly of block copolymers, where the interplay of enthalpic and entropic contributions to the free energy of the system determines the equilibrium morphology. To this end, linear block copolymers have provided well-ordered nanomaterials with domain spacings in the range of 5−50 nm, whereas domain spacings larger than 100 nm require significantly longer polymer chains.[3] However, difficulties in the synthesis or chain entanglements impede the formation of well-defined periodic morphologies, even in the presence of a large thermodynamic microphase segregation driving force between different segments or the use of chemical additives.[4,5] Contrary to linear block copolymers, bottle-brush block copolymers[6] have shown an exquisite ability of self-assembling into nanostructures with domain spacings well above 100 nm both in bulk and thin films.[7−9] Clearly, this unique behavior is attributed to the low entanglement density of the chains, because backbones of bottle-brush macromolecules are considerably stretched due to the presence of short side chains.[10,11] Additionally, these materials do not contain dyes and can be fabricated from organic polymers as, for example, in the manufacturing of photonic crystals[12] enabling the tuning of optical properties, or in the case of nanoporous membranes by serving as precursors for nanoporous materials with highly tunable cylindrical pore diameters.[13] Hence, the role of molecular architecture is a key element in controlling morphologies of nanomaterials, and, as a result, their properties.

Recently, computer simulations have provided evidence that bottle-brush copolymers self-assemble into lamellar structures, when the length of all side chains, irrespective of their type, is the same.[9] Moreover, an experimental study[13] has obtained morphologies with cylindrical domains, when both the volume fraction and length of the side chains of each type differ. Namely, the asymmetry in molecular composition induces an overall molecular asymmetry that favors the formation of cylindrical domains. Although this work has partly discussed different morphologies (i.e., lamellae and cylinders), the role of the molecular architecture in the self-assembly of bottle-brush copolymers requires further investigation.

In this study, we construct morphology diagrams of bottle-brush block copolymer melts by using Molecular Dynamics (MD) simulations of a bead−spring model (see Supporting Information). We demonstrate that the variation of the side chain lengths can lead to different morphologies, even when the volume fractions of the side chains of each component are equal. By exploring the possible parameter space, we find two-domain or three-domain morphologies, either lamellae or cylinders. Furthermore, we compare the obtained morphologies of bottle-brush copolymer melts with the respective linear triblock copolymer melts highlighting the differences between the two molecular architectures. Thus, we provide a comprehensive study on the equilibrium morphologies of compositionally symmetric bottle-brush block copolymer melts, anticipating that our results will provide a fundamental understanding required for the design of periodic soft materials based on the self-assembly of bottle-brush copolymer chains.

Our simulations are based on a standard bead−spring model (see Supporting Information), which was implemented in the large-scale atomic/molecular massively parallel simulator (LAMMPS[14]). Every bottle-brush block copolymer chain

**Received:** September 16, 2014
**Accepted:** October 8, 2014

   dx.doi.org/10.1021/mz500580f | ACS Macro Lett. 2014, 3, 1096−1100

contains three types of beads; letters A and B denote the different types of beads belonging to the side chains, while C denotes the backbone beads (Figure 1). We have only considered compositionally symmetric bottle-brush copolymers, which means that the total number of A and B beads is the same, that is, $M_A = M_B = M$, as well as the volume fractions ($f_A = f_B$). Moreover, grafted side chains of the same type always have the same length. Hence, by varying the length of the side chains ($N_A$ and $N_B$), the total number of backbone beads varies accordingly being $N_C = M/N_A + M/N_B$, because in our case, every side chain is attached to a single backbone bead. Thus, the volume fraction of the backbone beads, $f_C$, is not fixed with variation of the side chain length, but $f_C = 1 - f_A - f_B$. Hence, the obtained molecular architectures range from linear triblock copolymers (when $N_A = N_B = M$) to bottle-brush copolymers where each backbone bead is connected to one A- or B-type bead (Figure 1). In our study, the aspect ratios of our simulated macromolecules are rather low. However, larger aspect ratios not only would significantly increase the number of interaction centers per molecule but also the number of molecules to properly capture the self-assembly structures.

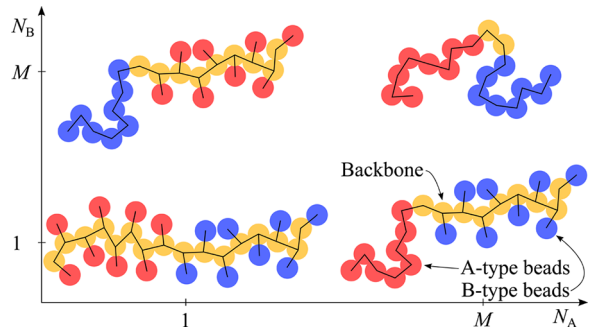


**Figure 1.** Schematic illustration of typical bottle-brush block copolymers for different length of A-type side chains ($N_A$) and B-type side chains ($N_B$). The total number for each type of side chain beads for each bottle-brush copolymer chains is equal to $M = 8$. The lengths of the same type of the side chains are equal. Thus, the top left and bottom right cases are equivalent due to the symmetric choice of interactions (see Supporting Information).

Our bottle-brush chains, being all of the same architecture for each simulation, are placed in a cubic simulation box with periodic boundary conditions applied in all directions. The *NPT* statistical ensemble is used, where the chosen pressure $P$ corresponds to the ambient pressure, and the temperature of the system is such to enable microphase separation between A- and B-type beads for given interaction parameters. Moreover, the phase separation is mainly driven by the incompatibility between A- and B-type beads, as none of the A or B beads has an energetic preference for the backbone beads. The map between the degree of segregation and the molecular parameters, which is expressed by the Flory−Huggins parameter $\chi$,[15] has been discussed recently.[16] In our study, the $\chi_{AB}$ effective parameter for A- and B-type beads is between 16 and 40, depending on the molecular weight, which corresponds to the intermediate segregation regime.[3] In this regime, we are able to obtain well-defined morphologies.

Due to the symmetric choice of interactions, various molecular architectures (e.g., bottom right and top left cases in Figure 1) are equivalent. Hence, the amount of simulations required for a full exploration of the parameter space based on the side chain lengths $N_A$ and $N_B$ (Figure 1) is significantly reduced (open vs full symbols in Figure 2a). Also, the symmetry in composition and interactions between beads ensures that most of the observed effects would be attributed to the molecular architecture. Indeed, the molecular architecture plays a significant role even in the self-assembly of diblock copolymer chains, where the final morphology is dictated by the relative sizes of their blocks,[3] as well as the intrinsic stiffness of the chain.[17] On the other hand, the stiffness of the backbone in bottle brush copolymers is induced by the presence of side chains[18] contributing significantly to the formation of the final morphology.

We find that bottle-brush copolymers with symmetric composition and interactions between A and B beads form either cylindrical (e.g., Figure 2, C16/C64) or lamellar (e.g., Figure 2, L16/L64) morphologies. The morphologies can be two- or three-domain morphologies (e.g., Figures 2 and 3) depending on the existence of a thin layer consisting of C backbone beads. The formation of cylinders occurs when the length of one type of side chains is equal to $M$, while the length of the other type of side chains is $N_B < M/4$. When the side chains A and B have equal length, we observe lamellar structures in agreement with experimental findings.[9] Although in our simulations domain sizes depend on the molecular weight of the different blocks consistent with experimental results,[8] the impact of the side-chains molecular weight ($M$) on the morphologies was invariant suggesting that our findings be scalable to larger molecular weights.

The formation of (hexagonally stacked) cylinders is clearly attributed to the molecular asymmetry; in diblock copolymers, the minority block should have a volume fraction less than about 0.3.[19,20] In bottle-bush copolymers the molecular asymmetry is introduced by the molecular architecture, despite the fact that the two blocks driving the phase separation have equal volume fractions. For example, we observe the lamellae to cylinder crossover when one of the blocks has a side chain of length $N_A = M$. In this case, the side chains of the other block are significantly short, but they are grafted onto a long backbone (e.g., Figure 2, C16 and C64). In other words, the morphology change from lamellae to cylinders occurs when the number of B-type beads with their attached backbone beads deviates significantly from the number of beads of the single A-type side chain with its attached backbone bead. As a result the backbone beads mixed with the B-type beads effectively increase the size of the B-block (Figure 3a) with the volume fraction of the beads surrounding the cylinders being $f_B + f_C$. This molecular asymmetry results in the formation of cylindrical domains. Due to our choice of keeping the volume fractions of A and B chains equal, as well as the length of each side chain of the same type, the molecular asymmetry between the two blocks occurs for $M/N_B = 4$ and $N_A = M$. This requirement deviates significantly from the typical volume fraction characterization on which block copolymers are based. For $N_B = 1$ ($M = 16$, Figure 2) the change from cylindrical to lamellar morphology occurs when $N_A$ changes from 8 to 16 beads, resulting in a change in the volume fraction of the backbone beads $f_C$ from 0.36 to 0.34, respectively. The same morphology crossover for $N_B = 2$ occurs for $N_A = 16$ to 8 corresponding to a different set of $f_C$ values, that is, $f_C = 0.24$ to 0.22, respectively. Therefore, the change in the volume fraction of the backbone beads is neither a sufficient condition for the cylinder formation nor does explain the reason that this morphology occurs only when one of the blocks is a single chain, for example, $N_A = M$.


dx.doi.org/10.1021/mz500580f | *ACS Macro Lett.* 2014, 3, 1096−1100

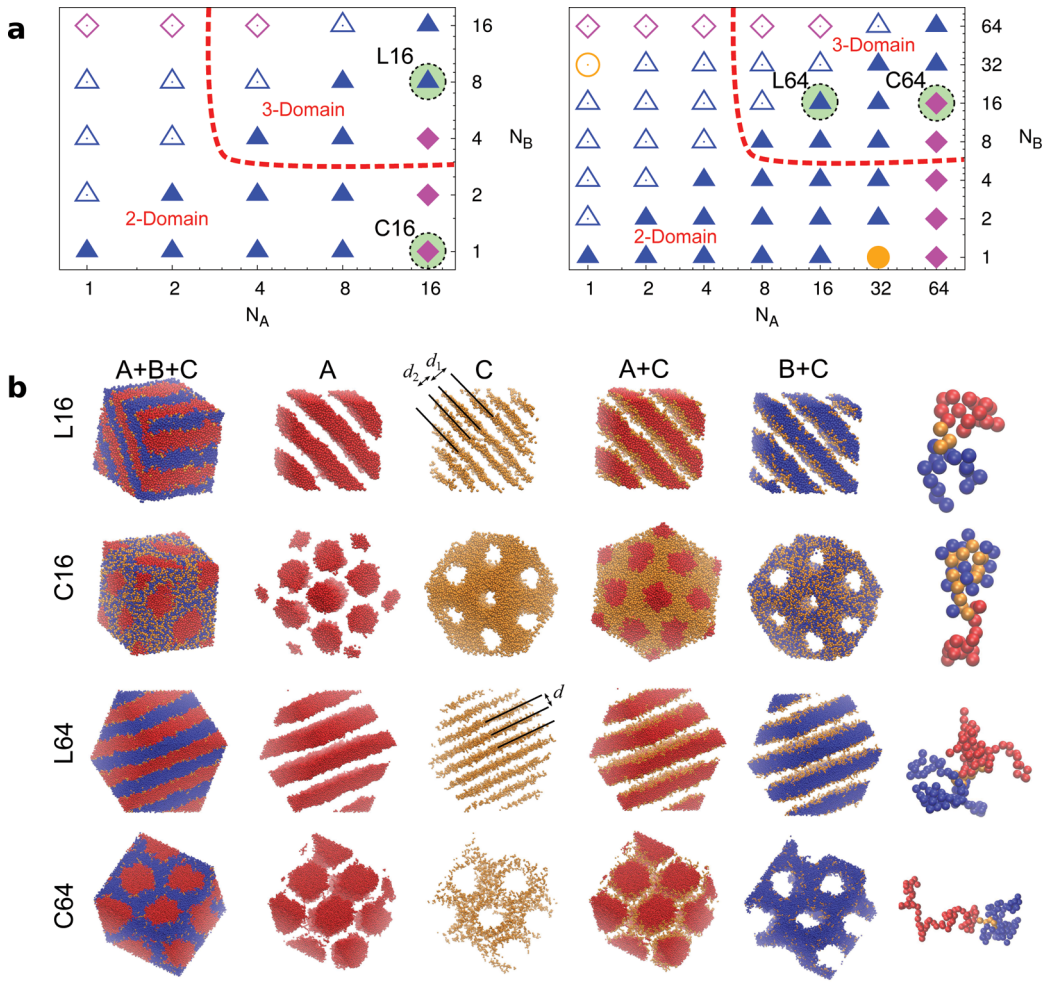


**Figure 2.** (a) Morphology diagrams for $M$ = 16 and 64 of bottle-brush block copolymers. Symbols correspond to different morphologies: lamellae (triangles), metastable (circles), and cylinders (diamonds). Open symbols correspond to symmetric cases of bottle-brush polymers, for which additional simulations were not required (see main text for details and Figure 1). The dashed line is an approximate boundary between the formation of two- (L16) and three-domain (C16) structures. (b) Snapshots of bottle-brush copolymer melts for selected systems as indicated; for each system we present different selection of domains for clarity. For L16 and L64 lines were drawn on the C-domains to illustrate the domain spacings, $d_1$ and $d_2$ for L16 and $d$ for L64. On the last column, typical molecular configurations of individual molecules as they appear inside the melt are presented.

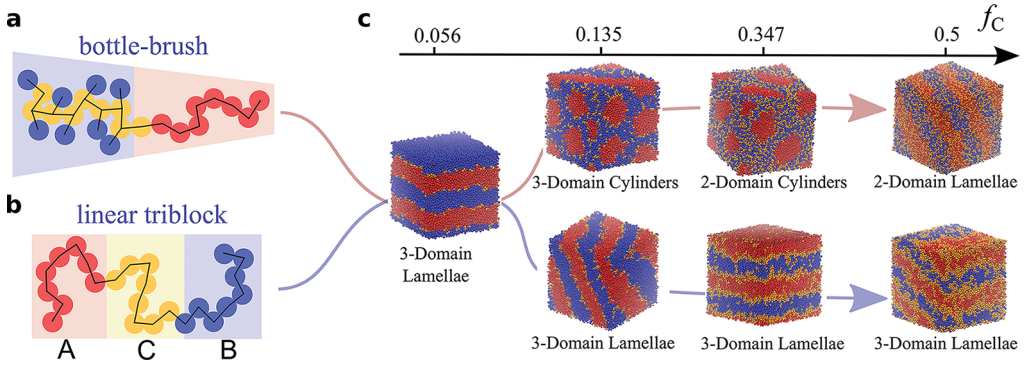


**Figure 3.** Schematic representation of bottle-brush (a) and linear ACB (b) triblock copolymer molecular architectures symmetric in composition. (c) Different morphologies obtained with variation of the volume fraction of the backbone beads, $f_C$ and $M$ = 16. ABC linear triblock copolymers also form three-domain lamellar structures (see Supporting Information).

A plausible explanation is that entropy may drive the self-assembly from cylinder to lamellar morphologies. In cylindrical structures of linear diblock copolymers, the minority block is more stretched than the majority block, leading to a free energy entropic penalty.[21] Assuming a valid analogy between cylinders formed by diblock and bottle-brush copolymers, the morphology behavior could be rationalized in terms of the molecular parameters. Increasing by one bead the backbone from the side of the block that forms a cylinder, it would reduce the side chain length by half. Hence, shorter chains would have to


dx.doi.org/10.1021/mz500580f | ACS Macro Lett. 2014, 3, 1096−1100

stretch significantly to satisfy the incompressible criterion in the case of cylinders. However, the stretching of a polymer chain reduces the total number of possible molecular configurations and since shorter chains have a smaller number of possible molecular configurations, it results in a higher entropic penalty.[22] In other words, the reduction of the side chain length would impose a large entropy penalty and it is enough to trigger a morphology crossover from cylinders to lamellae. Thus, in our work, the formation of cylinders is achieved for compositionally symmetric bottle-brushes, while a similar result was obtained experimentally[13] based on the asymmetry of molecular shape and volume fractions of the blocks, where the molecular aspect ratio was larger than the one used in our study.

The observed morphologies for compositionally symmetric bottle-brush copolymers may be two- or three-domain. In the case of three-domain lamellar morphologies, the backbone beads form a thin layer between the A- and B-type domains leading to a distinguished block sequence -A-C-B-C-A- (Figure 2, L16 and L64). The size of A- and B-domains is equal (because $f_A = f_B$) and increases with the molecular weight, in agreement with previous simulation and experimental studies.[8] The number of C-domains is equal to that of A- and B-domains, since the C-domains are located at the interfaces between the A- and B-domains (Figure 2, L64). Additionally, when the length of the side chains of the A- and B-blocks differs, two distinct domain spacings for the C-domains manifest (Figure 2, L16). To the best of our knowledge, this subtle effect has not been reported before. Clearly, it demonstrates that asymmetry in side chain lengths even when $f_A = f_B$ can be used to tune the domain spacing of the third domain, that is, C-domain. The three-domain morphologies form for small backbone volume fraction, $f_C$ (Figure 2 a). As $f_C$ continues to increase the C-domains start to merge into a single domain. In this way, two-domain lamellar morphologies form, where backbone beads mix with one or both of the A- and B-blocks (Figure 3c). Additionally, such two-domain morphologies form when at least one of the types of the side chains has a relatively short length, that is, $N_i \leq 2.6 \log M$, where $i$ refers to types A and B. Furthermore, we observe a similar behavior for cylinder morphologies. For two-domain cylinders, the A-type blocks form cylinders, while the surrounding matrix is filled with the backbone and the B-type segments (Figure 2, C16). On the other hand, in the case of the three-domain cylinders, the backbone segments form a thin layer around the cylinders (Figure 2, C64). These results indicate the broad range of design possibilities to guide the self-assembly process into different morphologies.

To highlight the differences between bottle-brush copolymers and linear copolymers, we compare the obtained morphologies based on those two molecular architectures (Figure 3 and Supporting Information). Because the interactions between beads are the same in both cases, differences may be mainly attributed to the molecular architecture. In linear triblock copolymers, the sequence of the blocks, that is, ABC or ACB, affects the formation of structures.[23] A wide range of "complex" structures emerge from the relative size of the blocks, while the asymmetry of energetic interactions enables the formation of a wider range of distinct structures.[24,25] Our investigation is similar to that of ref 26, where a morphology diagram of a triblock copolymer was constructed by keeping the volume fractions of A and B blocks equal while varying the size of the third block. A number of complex morphologies and a large variation of the order–disorder transition temperature were discussed. In our study, the triblock copolymers, symmetric in A and B volume fractions, always form three-domain lamellar structures, independently of the sequence of the blocks (Figure 3 and Supporting Information). The difference between the obtained morphologies in this study and those of ref 26 lie in the choice of the interaction parameters. Moreover, we find that the ACB linear triblock copolymer melts are able to reach the lamellar equilibrium morphology faster than the corresponding melts based on ABC triblock copolymer chains. Generally, there are two ways of increasing $f_C$ in bottle brush copolymers. The first way is to increase the backbone sequentially for both A- and B-blocks, which would result in the formation of lamellar structures (i.e., moving from the top right corner of the morphology diagrams of Figure 2 to the bottom left corner). For the same range of $f_C$, one may also attempt to increase the backbone of one of the blocks until the side chain consists of one bead and then increase the backbone for the second block (i.e., moving from the top right corner of the morphology diagrams of Figure 2a to the bottom left corner through configurations of the bottom right corner). Thus, the contrast between the linear triblock copolymers and bottle-brush copolymers reflects clearly the unique design potential of generating complex multidomain morphologies in a robust and scalable way.

In summary, our work illustrates the unique possibilities that bottle-brush copolymers offer in the design of novel soft self-assembly structures. By considering the side chains having equal volume fractions, we demonstrate that a variety of lamellar structures and hexagonally packed cylinders form with variation of molecular architecture. The cylinder formation is counterintuitive, because the molecular asymmetry required for the formation of cylindrical domains is driven by the asymmetry of the side chains length despite the volume fractions of the brushes being equal. This behavior has not been previously reported and we expect that our work will stimulate further investigations on morphology design based on the self-assembly of bottle-brush copolymers. Additionally, we find that bottle-brush copolymers offer a broad range of pathways of manufacturing in a robust way two- and three-domain lamellar and cylinder morphologies with faster self-assembly kinetics than linear triblock copolymer melts. In this respect, our work may offer new venues toward a more efficient design of morphologically well-defined periodic nanomaterials required for bespoke applications.

## ■ ASSOCIATED CONTENT

### Supporting Information

Further details on the methods and additional results. This material is available free of charge via the Internet at http://pubs.acs.org.

## ■ AUTHOR INFORMATION

### Corresponding Author

*E-mail: a.chremos@imperial.ac.uk.

### Notes

The authors declare no competing financial interest.

## ■ ACKNOWLEDGMENTS

The authors thank Imperial College London for providing computational resources.

## REFERENCES


(1) Meng, F.; Zhong, Z.; Feijen, J. *Biomacromolecules* **2009**, *10*, 197−209.
(2) Ruiz, R.; Kang, H.; Detcheverry, F. A.; Dobisz, E.; Kercher, D. S.; Albrecht, T. R.; de Pablo, J. J.; Nealey, P. F. *Science* **2008**, *321*, 936−939.
(3) Bates, F. S. *Science* **1991**, *251*, 898−905.
(4) Kang, Y.; Walish, J. J.; Gorishnyy, T.; Thomas, E. L. *Nat. Mater.* **2007**, *6*, 957−960.
(5) Urbas, A.; Sharp, R.; Fink, Y.; Thomas, E. L.; Xenidou, M.; Fetters, L. J. *Adv. Mater.* **2000**, *12*, 812−814.
(6) Walther, A.; Muller, A. H. *Chem. Rev.* **2013**, *113*, 5194−261.
(7) Rzayev, J. *Macromolecules* **2009**, *42*, 2135−2141.
(8) Hong, S. W.; Gu, W.; Huh, J.; Sveinbjornsson, B. R.; Jeong, G.; Grubbs, R. H.; Russell, T. P. *ACS Nano* **2013**, *7*, 9684−9692.
(9) Gu, W.; Huh, J.; Hong, S. W.; Sveinbjornsson, B. R.; Park, C.; Grubbs, R. H.; Russell, T. P. *ACS Nano* **2013**, *7*, 2551−2558.
(10) Vlassopoulos, D.; Fytas, G.; Loppinet, B.; Isel, F.; Lutz, P.; Benoit, H. *Macromolecules* **2000**, *33*, 5960−5969.
(11) Hu, M.; Xia, Y.; McKenna, G. B.; Kornfield, J. A.; Grubbs, R. H. *Macromolecules* **2011**, *44*, 6935−6943.
(12) Sveinbjornsson, B. R.; Weitekamp, R. A.; Miyake, G. M.; Xia, Y.; Atwater, H. A.; Grubbs, R. H. *Proc. Natl. Acad. Sci. U.S.A.* **2012**, *109*, 14332.
(13) Bolton, J.; Bailey, T. S.; Rzayev, J. *Nano Lett.* **2011**, *11*, 998−1001.
(14) Plimpton, S. J. *J. Comput. Phys.* **1995**, *117*, 1.
(15) Flory, P. J. *Principles of Polymer Chemistry*; Cornell University Press: Ithaca, NY, 1953.
(16) Chremos, A.; Nikoubashman, A.; Panagiotopoulos, A. Z. *J. Chem. Phys.* **2014**, *140*, 054909.
(17) Singh, C.; Goulian, M.; Liu, A. J.; Fredrickson, G. H. *Macromolecules* **1994**, *27*, 2974−2986.
(18) Theodorakis, P. E.; Hsu, H.-P.; Paul, W.; Binder, K. *J. Chem. Phys.* **2011**, *135*, 164903.
(19) Matsen, M. W.; Schick, M. *Phys. Rev. Lett.* **1994**, *72*, 2660−2663.
(20) Khandpur, A. K.; F oster, S.; Bates, F. S.; Hamley, I. W.; Ryan, A. J.; Bras, W.; Almdal, K.; Mortensen, K. *Macromolecules* **1995**, *28*, 8796−8806.
(21) Birshtein, T. M.; Zhulina, E. B. *Polymer* **1989**, *30*, 170−177.
(22) Rubinstein, M.; Colby, R. H. *Polymer Physics*; Oxford University Press: Oxford, 2003.
(23) Tang, P.; Zhang, H.; Yang, Y. *Phys. Rev. E* **2004**, *69*, 031803.
(24) Bates, F. S.; Hillmyer, M. A.; Lodge, T. P.; Bates, C. M.; Delaney, K. T.; Fredrickson, G. H. *Science* **2012**, *336*, 434−340.
(25) Beckingham, B. S.; Register, R. A. *Macromolecules* **2013**, *46*, 3486−3496.
(26) Bailey, T. S.; Pham, H. D.; Bates, F. S. *Macromolecules* **2001**, *34*, 6994−7008.